Inorganic Chemistry

Article

pubs.acs.org/IC

Redox and Luminescent Properties of Robust and Air-Stable N-Heterocyclic Carbene Group 4 Metal Complexes

Charles Romain,[†] Sylvie Choua,[†] Jean-Paul Collin,[†] Martine Heinrich,[†] Corinne Bailly,[†] Lydia Karmazin-Brelot,[†] Stéphane Bellemin-Laponnaz,*[,‡,§] and Samuel Dagorne*[,†]

[†]Institut de Chimie de Strasbourg, CNRS UMR 7177, Université de Strasbourg, 1 rue Blaise Pascal, 67000 Strasbourg, France

[‡]Institut de Physique et Chimie des Matériaux de Strasbourg, CNRS UMR 7504, Université de Strasbourg, 23 rue du Loess BP43, 67034 Strasbourg, France

[§]Institute for Advanced Study, Université de Strasbourg, 5 allée du Général Rouvillois, 67083 Strasbourg, France

Supporting Information

ABSTRACT: Robust and air-stable homoleptic group 4 complexes of the type $M(L)_2$ [**1**−**3**; M = Ti, Zr, Hf; L = dianionic bis(aryloxide) N-heterocyclic carbene (NHC) ligand] were readily synthesized from the NHC proligand 1,3-bis(3,5-di-*tert*-butyl-2-hydroxyphenyl)-imidazolinium chloride (**H_3L,Cl**) and appropriate group 4 precursors. As deduced from cyclic voltammetry studies, the homoleptic bis-adduct zirconium and hafnium complexes **2** and **3** can also be oxidized, with up to four one-electron-oxidation signals for the zirconium derivative **2** (three reversible signals). Electron paramagnetic resonance data for the one-electron oxidation of complexes **1**−**3** agree with the formation of ligand-centered species. Compounds **2** and **3** are luminescent upon excitation in the absorption band at 362 nm with emissions at 485 and 534 nm with good quantum yields (ϕ = 0.08 and 0.12) for **2** and **3**, respectively. In contrast, the titanium complex **1** does not exhibit luminescent properties upon excitation in the absorption band at 310 and 395 nm. Complexes **2** and **3** constitute the first examples of emissive nonmetallocene group 4 metal complexes.

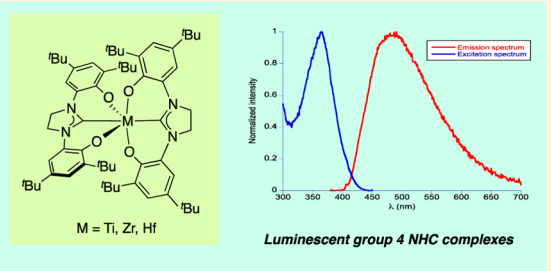

INTRODUCTION

Over the past 20 years, N-heterocyclic carbenes (NHCs) have become a ubiquitous class of ancillary ligands for coordination to transition-metal complexes with numerous applications in homogeneous catalysis[1−9] and medicinal, luminescent, and materials applications.[10,11] The use of NHC ligands for coordination to high-oxidation-state and early transition metals has been much less studied than the use of their late-transition-metal counterparts,[12,13] which is certainly ascribed to the presumed kinetic instability of the M−NHC bond upon coordination to oxophilic and electropositive metal centers. Aiming at robust NHC-supported high-oxidation-state metal complexes, we have developed tridentate bis(aryloxide) NHC chelating ligands (**A**) that form robust and stable early-transition-metal NHC-based chelate complexes,[14−17] with successful applications in polymerization catalysis.[15,17] In addition to their excellent chelating properties, tridentate ligands of type **A** may exhibit interesting redox properties because they contain electron-rich aryloxide groups typically known as redox "noninnocent" ligands.[18−22] In this regard, a few early-transition and high-oxidation-state metal complexes containing aryloxide moieties have been shown to be redox-active metal complexes,[23−26] leading to the mediation of various bond-activation processes[27,28] and group-transfer reactions.[29] In addition to their redox properties, a small number of high-oxidation-state d^0 transition-metal complexes with luminescent properties are known including, most notably, scandium,[30,31] tantalum,[32,33] and niobium[33] derivatives. Also, reports on group 4 species featuring luminescence properties are rare. In this area, group 4 metallocenes were shown to luminesce at low temperature (77 K),[34−36] with high quantum yield and long-lived excited state in some cases,[37] with such a luminescence being attributed to a ligand-to-metal charge-transfer (LMCT) state. Loukova et al. recently reported on a rigid zirconium-*ansa* metallocene dichloride being emissive at room temperature in solution.[38] Polyphenylzirconium and -hafnium metallocene complexes were demonstrated to be suitable luminophores for cell imaging at room temperature.[39]

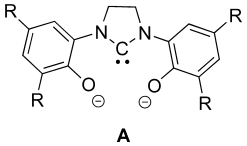

A

Here, we report on the synthesis, structural characterization, and redox behavior of a novel family of air-stable homoleptic NHC bis-adduct group 4 metal complexes that luminesce at room temperature in solution.[8,40−42]

Received: March 27, 2014
Published: June 24, 2014

   dx.doi.org/10.1021/ic500718y | *Inorg. Chem.* 2014, 53, 7371−7376

RESULTS AND DISCUSSION

Synthesis and Characterization of Homoleptic Complexes 1−3. The NHC protio ligand 1,3-bis(3,5-di-*tert*-butyl-2-hydroxyphenyl)imidazolinium chloride (**H_3L,Cl**) was prepared according to a literature procedure from *N*,*N*-bis(3,5-di-*tert*-butyl-2-hydroxyphenyl)ethylenediamine using a classical procedure [HCl and then $(EtO)_3CH$].[14] The direct reaction of the chloride salt species **H_3L,Cl** with 0.5 equiv of $TiCl_4(THF)_2$ or 0.5 equiv of MCl_4 (M = Zr, Hf) in the presence of NEt_3 (6 equiv) led to the formation of the corresponding homoleptic bis-adduct group 4 metal complexes $M(L)_2$ (**1**−**3**; M = Ti, Zr, Hf) , all isolated in high yield (Figure 1 and the Experimental Section).

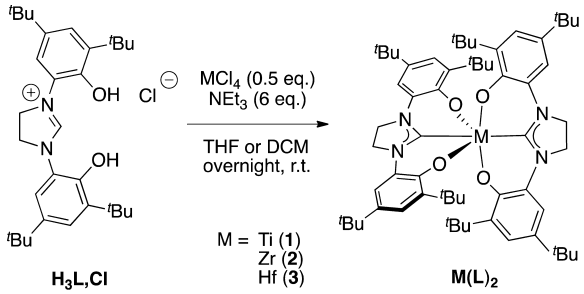

Figure 1. Synthesis of homoleptic NHC bis-adduct group 4 metal complexes **1**−**3**.

The NMR data for complexes **1**−**3** agree with an effective C_{2v} symmetry in solution (Figures S1−S4 in the Supporting Information, SI) under the studied conditions (CD_2Cl_2, room temperature) and feature a characteristic ^{13}C NMR carbene signal at δ 200.0, 200.8, and 206.1 for complexes **1**−**3**, respectively.[43] All three homoleptic bis-adduct group 4 metal complexes are air-stable either in the solid state or in solution, which is certainly related to the steric protection of the metal center[23] and reflects the excellent stability of the formed group 4 metal (OCO)M chelates.

The solid-state molecular structure of complexes **1**−**3**, as determined by X-ray crystallography, unambiguously confirmed the bis-adduct nature of species **1**−**3** (see Figures 2 and 3 for

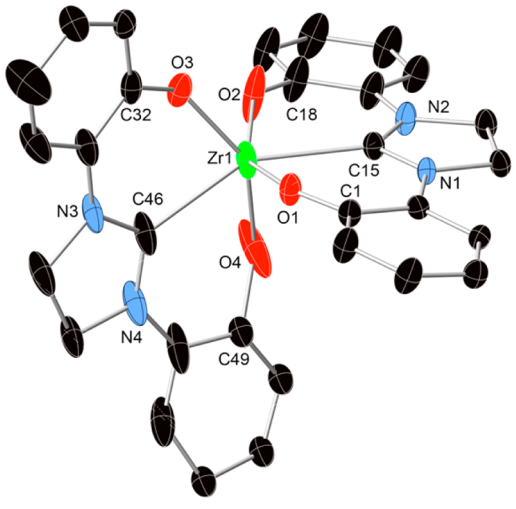

Figure 2. X-ray structure of zirconium complex **2** (ORTEP view, 50% probability ellipsoids). ^{t}Bu and hydrogen atoms were omitted for clarity.

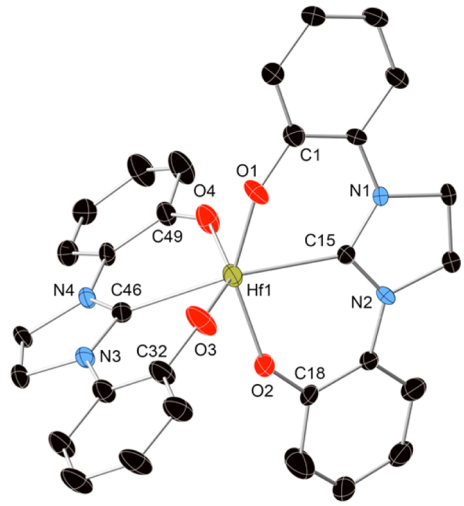

Figure 3. X-ray structure of hafnium complex **3** (ORTEP view, 50% probability ellipsoids). ^{t}Bu and hydrogen atoms were omitted for clarity.

complexes **2** and **3**, respectively; for the molecular structure of **1**, see ref 16). In all three complexes, the group 4 metal center adopts a distorted octahedral geometry resulting from the *mer* coordination of two OCO^{2-} chelating ligands, so that the NHC donors are *trans* to one another. The zirconium and hafnium complexes **2** and **3** show similar metrics (see the selected bond lengths and angles in Table 1) with [OCO−M] chelate

Table 1. Selected Data from Molecular Structures 1−3

	1	2	3
	Bond Length (Å)		
M−C15	2.233(2)	2.379(2)	2.357(6)
M−C46	2.222(2)	2.387(3)	2.351(6)
M−O1	1.897(1)	2.007(2)	1.999(4)
M−O2	1.872(1)	2.014(2)	2.005(5)
M−O3	1.909(2)	2.011(2)	2.001(5)
M−O4	1.908(2)	2.007(3)	2.002(5)
	Angle (deg)		
C15−M−O1	79.80(7)	75.49(7)	77.2(2)
C46−M−O3	79.21(7)	76.4(1)	76.6(2)
O1−M−O2	155.48(7)	146.3(1)	146.6(2)
O3−M−O4	157.20(6)	146.6(1)	147.3(2)
	Dihedral Angle (deg)		
C32−O3−O4−C49	65.6(2)	0.6(5)	12.5(9)
C1−O1−O2−C18	47.2(2)	8.0(4)	11(1)

moieties (M = Zr, Hf) slightly distorted from planarity (C1−O1−O2−C18 = 8.0° and 11° for **2** and **3**, respectively), in line with similar ionic radii (Zr^{IV} = 86 pm and Hf^{IV} = 85 pm).[33] Both complexes show M−$C_{carbene}$ bond lengths (see Table 1) in the range of related chelating NHC−M (M = Zr, Hf) complexes.[44−46] In contrast, the titanium complex **1** exhibits significantly distorted [OCO−Ti] chelate moieties (C1−O1−O2−C18 = 47.2°) and a rather long Ti−$C_{carbene}$ bond relative to previously reported OCO−Ti complexes,[16] which is presumably due to steric hindrance around the titanium metal center (ionic radius Ti^{IV} = 74.5 pm).[33]

Electrochemical Properties of Complexes 1−3. The electrochemical properties of group 4 metal complexes **1**−**3** were studied by cyclic voltammetry (CV) and potential-controlled electrolysis in dichloromethane containing 0.10 M

dx.doi.org/10.1021/ic500718y | Inorg. Chem. 2014, 53, 7371−7376

tetra-*n*-butylammonium hexafluorophosphate as the supporting electrolyte (see the Experimental Section). Under the studied conditions, the homoleptic bis-adduct titanium complex **1** can be readily oxidized. As depicted in Figure 4, two similar and

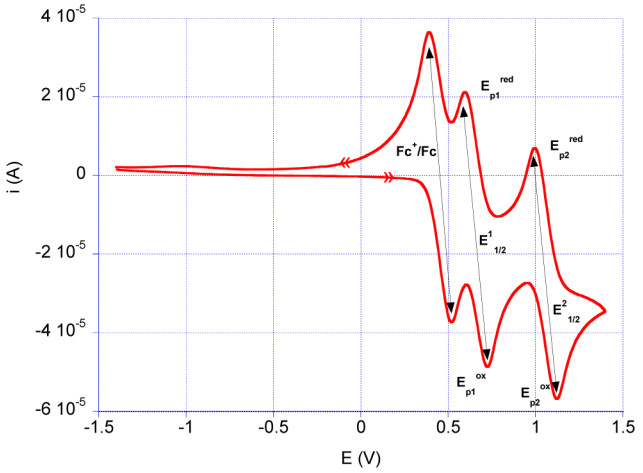

Figure 4. CV of complex **1** (0.1 mM, CH_2Cl_2, with Fc) recorded at a 100 mV/s scan rate (buffer: 0.1 M NBu_4PF_6).

reversible redox couples located at $E^1_{1/2}$ = 0.68 V and $E^2_{1/2}$ = 1.08 V are observed. The coulometric oxidation at 0.70 V for species **1** yielded a flow of current of 1.07 faraday/mol, thus indicating that the wave at 0.68 V corresponds to a one-electron oxidation. Owing to the similarity of the two reversible CV signals, it may be assumed that the second wave at 1.08 V also corresponds to a one-electron oxidation. These potential values (0.21 and 0.61 V vs Fc^+/Fc; see the Experimental Section) lie within the range of related oxidation potentials observed for d^0 metal complexes bearing aryloxide ligands [0.33−1.04 V vs Fc^+/Fc],[21,23,24] suggesting an aryl-based oxidation. Under identical CV conditions, it is worth noting that the imidazolinium salt proligand $\mathbf{H_3L,PF_6}$ exhibited no signal (Table 2).

Table 2. Redox Potentials (V) for Complexes 1−3[a]

compound	$E^1_{1/2}$ (ΔE_{p1})	$E^2_{1/2}$ (ΔE_{p2})	$E^3_{1/2}$ (ΔE_{p3})	$E^4_{1/2}$
1	0.68 (0.12)	1.08 (0.12)		
2	0.79 (0.08)	1.11 (0.12)	1.38 (0.13)	1.76*
3	0.80 (0.18)	1.15 (0.18)	1.47*	
$\mathbf{H_3L,PF_6}$				

[a]Conditions: [complex] = 1.0 mM in CH_2Cl_2 (0.1 M NBu_4PF_6), scan rate 100 mV/s, and ferrocene (Fc) used as an internal standard. The potentials are referenced versus SCE: $E_{1/2} = (E_p^{ox} + E_p^{red})/2$ for reversible one-electron-transfer processes; $\Delta E_p = (E_p^{ox} - E_p^{red})$; (*) oxidation peak potentials E_p^{ox} for irreversible processes.

As deduced from CV studies, the homoleptic bis-adduct zirconium and hafnium complexes **2** and **3** can also be oxidized with up to four one-electron-oxidation signals for the zirconium derivative **2** (three reversible signals) and up to three oxidation signals (two reversible signals) for the hafnium complex **3** (see Figures S7−S10 in the SI). The values of the redox potentials are indicated in Table 2.

The three homoleptic bis-adduct complexes exhibit a somewhat similar electrochemical behavior, with each of them featuring two reversible one-electron-transfer waves. The observed sequential oxidations are consistent with the successive formation of phenoxyl radicals, with up to four one-electron steps for the zirconium complexes (one per aryloxide group). The excellent reversibility of the signals may be due to the presence of steric protection induced by the bulky ^{t}Bu group in the ortho and para positions. It is worth noting that zirconium and hafnium complexes **2** and **3**, which feature similar metrics (see Table 1), do exhibit nearly identical redox potentials but noticeably different from those of the titanium complex analogue **1**. Such a behavior was earlier observed by Wieghardt and co-workers with a series of isostructural complexes of type $M^{III}L$ (M = Co^{III}, Cr^{III}, Fe^{III}, Ga^{III}, and Sc^{III}) featuring metal-ion-dependent redox potentials for the first oxidation of the same ligand.[23]

To characterize the nature of the one-electron oxidation of complexes **1**−**3**, X-band electron paramagnetic resonance (EPR) spectra of the oxidation products of **1**−**3**, with the latter species being in situ generated at room temperature by potential-controlled experiments in CH_2Cl_2 with 0.1 M ^{n}Bu_4NPF_6 as the supporting electrolyte (see the Experimental Section), were recorded. When electrolysis is conducted on the first potential oxidation, a single narrow line is only observed for all three complexes (Figure 5). Isotropic *g* values (~2.00) are close to the free electron. The peak-to-peak line widths of signals **1**−**3** were estimated to be 8, 7, and 11 G, respectively.

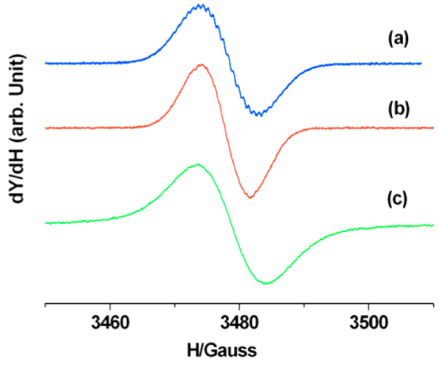

Figure 5. EPR spectra after electrolysis at room temperature of complexes **2** (a), **1** (b), and **3** (c).

The shape of the lines suggests that some unresolved hyperfine couplings and motion effects cause a broadening of the signals. Nevertheless, by decreasing the modulation amplitude by up to 0.2 G, the EPR signal for **2** is resolved. The latter spectrum (see Figure S11 in the SI) could be simulated by using two different spin nuclei: two sets of four protons with a coupling constant A_{iso} = 1.37 and 0.61 G and one set of four nitrogen atoms with a coupling constant of A_{iso} = 2.32 G. These data are consistent with a ligand-centered radical species. Note that all generated radical species are stable at room temperature under an argon atmosphere even after a large increase of the voltage. Identical EPR data were recorded by chemical oxidation with $AgSbF_6$.

Optical Properties of Complexes 1−3. The optical properties of the NHC group 4 complexes **1**−**3** and their potential luminescent properties were also investigated (Figures 6 and 7 and S13−15 in the SI). The UV−visible absorption spectrum of the titanium complex **1** exhibits intense absorption bands for $\lambda < 310$ nm ($\varepsilon > 10^4$ M^{-1} cm^{-1}; Table 3) assigned to ligand-based transitions[24] (see Figure S12 in the SI for the UV−visible absorption spectrum of the ligand precursor

dx.doi.org/10.1021/ic500718y | Inorg. Chem. 2014, 53, 7371−7376

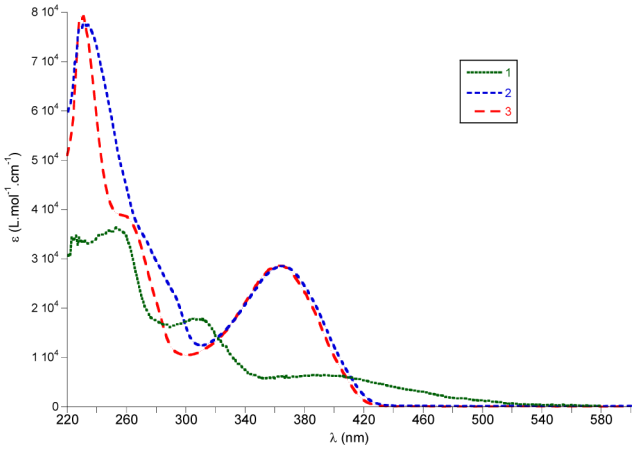

Figure 6. UV−visible absorption spectra of **1**−**3** in CH_2Cl_2 (1×10^{-5} M) at 25 °C.

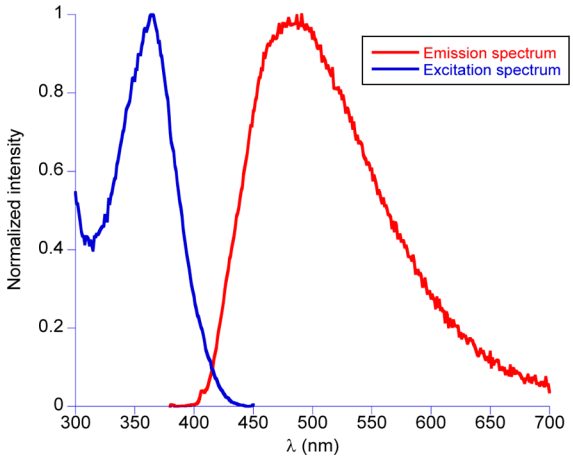

Figure 7. Excitation spectrum (λ_{em} = 485 nm) and emission spectrum (λ_{ex} = 362 nm) of compound **2** in CH_2Cl_2 at 25 °C.

Table 3. Selected Electronic Transitions for 1−3

	LMCT absorption			luminescence	
complex	λ_{max} (nm)	E_{LMCT} (eV)	ϵ (M^{-1} cm^{-1})	λ (nm)	ϕ
1	394	3.147	6500		
2	366	3.388	28600	485	0.08
3	365	3.397	28700	534	0.12

H_3L,Cl). The lower-energy broad band at 394 nm ($\varepsilon \approx 6500$ M^{-1} cm^{-1}) was ascribed to an aryloxide-to-titanium charge-transfer (LMCT) transition, with a tail in the visible explaining the intense red color of the titanium complex in solution. Similar LMCT transitions were previously observed for tris(aryloxide) titanium complexes bearing variously substituted aryloxide moieties.[24] For instance, the absorption peak at 366 nm for a tris(di-*tert*-butyl)phenoxide titanium acetate complex[24] was attributed to an aryloxide-to-titanium LMCT transition. The UV−visible absorption spectra of the zirconium and hafnium complexes **2** and **3** show intense absorption bands for $\lambda < 300$ nm ($\varepsilon > 4 \times 10^4$ M^{-1} cm^{-1}) assigned to intraligand transitions and an intense LMCT-type transition around 365 nm ($\varepsilon \approx 2.8 \times 10^4$ M^{-1} cm^{-1}) assigned by analogy with the UV−visible absorption data for the titanium species **1**. The influence of the metal center on LMCT transitions [i.e., in the present case, the shift to lower energy for the titanium complex **1** (λ = 395 nm) versus zirconium and hafnium complexes **2** and **3** (λ = 365 nm)] was previously observed for group 4 metallocenes and rationalized by a weaker ligand−metal interaction for the titanium derivatives.[46] In the case of species **2** and **3**, the similar LMCT transitions along with nearly identical metrics in the solid state (Figures 2 and 3) suggest a comparable overlap of the ligand orbitals with metal d orbitals in both complexes.

Luminescence analyses demonstrated that compounds **2** and **3** luminesce upon excitation in the LMCT absorption band (λ_{ex} = 362 nm) with emissions at 485 and 534 nm with good quantum yields of ϕ = 0.08 and 0.12 (for **2** and **3**, respectively). The excitation spectra of **2** and **3** only contain one band at 362 nm, in accordance with the absorption spectra (Figures S13−S15 in the SI). Thus, the peaks are Stokes-shifted from 6706 and 8670 cm^{-1} (relative to the excitation peak) for **2** and **3**, respectively. Importantly, no luminescence was observed for complexes **2** and **3** under aerobic conditions (Figures S18 and S19 in the SI), indicative of a triplet emission being quenched by $^3O_2$. Time-resolved studies concluded on a very short lifetime of the excited state, in the range of nanoseconds, for complexes **2** and **3** (Figures S16 and S17 in the SI). Note that relatively short luminescence lifetimes (triplet emission; lifetimes up to 5−10 ns in degassed solutions) were recently reported for a family of polyphenylzirconium(IV) and -hafnium(IV) metallocenes.[39]

In contrast, the titanium complex **1** shows no luminescence properties upon excitation at 310 and 394 nm in the investigated conditions (room temperature, dichloromethane). Overall, the present data are in line with an earlier study on a series of luminescent metallocene group 4 complexes concluding on a significant increase of the luminescence quantum yield upon going from titanium(IV) to zirconium(IV)/hafnium(IV) derivatives.[45]

SUMMARY AND CONCLUSION

In summary, three new robust NHC-containing group 4 metal homoleptic complexes of the type OCO−M (M = Ti, Zr, Hf) were shown to be redox-active and, in the case of the zirconium and hafnium species, to be luminescent. These complexes exhibit up to four reversible redox signals, and, interestingly, the generated radical cations (arising from oxidation) are thermally stable under argon. Given the potential utility of OCO−M-type species (M = group 4 metal) in catalysis,[15−17] the present work may open the way to novel redox-tuned NHC group 4 catalysts. Preliminary studies of the optical properties of the NHC species agree with the luminescence properties in solution at room temperature, with these constituting the first examples of emissive nonmetallocene group 4 metal complexes. Further studies in the area will focus on the use of such redox-active NHC complexes in catalysis as well as on ligand modulations and computational studies for a thorough understanding of these systems.

EXPERIMENTAL SECTION

General Considerations. All experiments were carried out under dinitrogen using standard Schlenk techniques or in an MBraun Unilab glovebox. Tetrahydrofuran (THF), dichloromethane, and pentane were first dried through a solvent purification system (MBraun SPS) and stored for at least a couple of days over activated molecular sieves (4 Å) in a glovebox prior to use. CD_2Cl_2 and C_6D_6 were purchased from Eurisotop (CEA, Saclay, France), degassed under a dinitrogen flow, and stored over activated molecular sieves (4 Å) in a glovebox

dx.doi.org/10.1021/ic500718y | Inorg. Chem. 2014, 53, 7371−7376

prior to use. All other chemicals were used as received. NMR spectra were recorded on Bruker AC 300 and 400 MHz NMR spectrometers, in Teflon-valved J. Young NMR tubes at ambient temperature, unless otherwise indicated. ^{1}H and ^{13}C chemical shifts are reported versus $SiMe_4$ and were determined by reference to the residual ^{1}H and ^{13}C solvent peaks. Mass spectra were recorded by the "service de masse" of the Chemistry Department, University of Strasbourg. High-resolution mass spectromtery (HRMS) experiments were performed on a Bruker Daltonics microTOF spectrometer (Bruker Daltonik GmgH, Bremen, Germany) equipped with an orthogonal electrospray (ESI) interface. Calibration was performed using Tunning mix (Agilent Technologies). Sample solutions were introduced into the spectrometer source with a syringe pump (Harvard type 55 1111: Harvard Apparatus Inc., South Natick, MA) with a flow rate of 5 μL min^{-1}. Elemental analyses for all compounds were performed at the Service de Microanalyse of the Université de Strasbourg. Single crystals of complexes were mounted on glass fibers and data collected on a Nonius Kappa CCD or Bruker APEX II DUO Kappa CCD area detector diffractometer (Mo Kα, λ = 0.71073 Å).

Preparation of Complexes 1−3. *Ti(L)$_2$ (1).* A THF solution (5 mL) of $TiCl_4(THF)_2$ (81.0 mg, 0.243 mmol) was added to a stirring solution of the imidazolinium salt $\mathbf{H_3L}$ (250.0 mg, 0.485 mmol) in THF (20 mL). The solution immediately turned red after the addition of the titanium reagent. Then, NEt_3 (203 μL, 1.46 mmol) was added. The solution turned to dark red/brown, and slowly a precipitate formed. The solution was stirred overnight at room temperature and then evaporated to dryness to afford a dark-red/brown solid residue. In a glovebox, dry toluene (30 mL) was added to the latter residue to yield a red suspension, which was filtered under vacuum through Celite in a glass frit. Evaporation of this toluene solution in vacuo and washing with pentane afforded pure **1** as a red solid, as deduced by NMR spectroscopy and elemental analysis.[16]

Zr(L)$_2$ (2). A CH_2Cl_2 solution (4 mL) of $ZrCl_4$ (45.2 mg, 0.194 mmol) was added at room temperature via a pipet to a stirring CH_2Cl_2 solution (15 mL) of the imidazolinium chloride salt $\mathbf{H_3L}$ (200.0 mg, 0.388 mmol). Then NEt_3 (0.203 mL, 1.46 mmol.) was added dropwise, and the initial colorless solution progressively turned yellow. The reaction mixture was stirred overnight at room temperature to yield a yellow/green solution. Evaporation to dryness, the subsequent addition of toluene, and filtration of the resulting suspension through Celite on a glass frit yielded species **2** as an analytically pure colorless solid after washing with pentane (187 mg, 92% yield). ^{1}H NMR (300 MHz, CD_2Cl_2): δ 7.01 (d, J = 2 Hz, 4H), 6.95 (d, J = 2 Hz, 4H), 4.37 (s, 8H), 1.32 (s, 36H), 1.10 (s, 36H). ^{13}C NMR (75 MHz, CD_2Cl_2): δ 200.8 (C_{quat}), 149.5 (C_{quat}, aryl), 138.7 (C_{quat}, aryl), 137.2 (C_{quat}, aryl), 130.0 (C_{quat}, aryl), 118.7 (CH, aryl), 111.9 (CH, aryl), 47.7 (CH_2, NCH_2), 35.0 (C_{quat}, ^{t}Bu), 34.3 (C_{quat}, ^{t}Bu), 31.5 (CH_3, ^{t}Bu), 29.2 (CH_3, ^{t}Bu). HRMS (ESI). Calcd for $[C_{62}H_{88}N_4O_4Zr + Na]^+$: m/z 1065.5745. Found: m/z 1065.588. Elem. anal. Calcd for compound **2**: C, 71.29; H, 8.48; N, 5.36. Found: C, 71.02; H, 8.70; N, 5.36.

Hf(L)$_2$ (3). The same procedure as that for **2** was used. ^{1}H NMR (300 MHz, CD_2Cl_2): δ 7.04 (d, J = 2 Hz, 4H), 6.95 (d, J = 2 Hz, 4H), 4.37 (s, 8H), 1.33 (s, 36H), 1.11 (s, 36H).[1] ^{3}C NMR (75 MHz, CD_2Cl_2): δ 206.1 (C_{quat}), 150.2 (C_{quat}, aryl), 139.0 (C_{quat}, aryl), 138.1 (C_{quat}, aryl), 130.5 (C_{quat}, aryl), 119.2 (CH, aryl), 112.2 (CH, aryl), 48.1 (CH_2, NCH_2), 35.4 (C_{quat}, ^{t}Bu), 34.7 (C_{quat}, ^{t}Bu), 31.9 (CH_3, ^{t}Bu), 29.6 (CH_3, ^{t}Bu). Elem. anal. Calcd for compound **3**: C, 65.79; H, 7.84; N, 4.95. Found: C, 65.99; H, 8.12; N, 4.66.

Physical Measurements. UV−visible absorption spectra were recorded with a Kontron Instruments UVIKON 860 spectrometer at room temperature with a 1 cm path cell. Luminescence spectra were recorded at room temperature using a Fluorolog FL3-22 spectrofluorometer (Horiba Jobin Yvon) equipped with a TBX-04 detector. All of the measurements were performed on optically dilute solutions, taken so that the maximum absorbance is 0.05 (in the range 1×10^{-5}−5×10^{-5} mol L^{-1}). In a glovebox, the solutions were introduced in a modified 1 cm quartz cell equipped with J. Young taps. Solvents were dried and degassed prior to use, as previously mentioned.

For the luminescence steady-state measurements, the spectrometer was equipped with a 450 W xenon lamp excitation source and excitation and emission double-grating monochromators with bandpasses set at 2 nm for the experiments. The spectra were corrected for the lamp, the monochromators, and the detector responses. The luminescence quantum yields were determined in dichloromethane solutions using quinine sulfate in aerated 0.05 M H_2SO_4 as a luminescence standard (Φ_{em} = 0.55).[41]

The luminescence decays were collected by a time-correlated single-photon-counting technique. The excitation source was a NanoLED-370 electroluminescent diode (Horiba Jobin Yvon) emitting at 375 nm and operated at a 1 MHz repetition rate. The bandpass of the emission double-grating monochromator was set at 2 nm for the measurements. The instrument response function was collected using a dilute scattering solution of Ludox (Sigma-Aldrich). The theoretical luminescence decays were assumed to be sums of two or three exponentials. They were iteratively reconvoluted with the measured instrument response prior to fitting with the measured luminescence decays using the least-squares method of Fluorescence Decay Analysis Software DAS6 (Horiba Jobin Yvon). The goodness of fit was evaluated by the X^2 criterion, the randomness of the residuals, and their autocorrelation.

CV measurements were performed with a three-electrode system consisting of a platinum working electrode, a platinum wire counter electrode, and a silver wire pseudoreference electrode. Ferrocene (Fc) was used as an internal reference. All redox potentials are referenced versus saturated calomel electrode (SCE) unless indicated otherwise (potentials referenced versus Fc will be noted "vs Fc^+/Fc"). In potential-controlled electrolysis, large platinum wires are used as working and counter electrodes. In this case, the counter electrode is separated from the electrolyte solution by a glass frit. The measurements were carried out at room temperature under argon, in degassed spectroscopic-grade solvents, using 0.1 M $^{n}Bu_4NPF_6$ solutions in CH_2Cl_2 as the supporting electrolyte. An EG&G Princeton Applied Research model 273A potentiostat connected to a computer was used (software from Electrochemistry Research).

EPR Experiments. EPR spectra were recorded with an ESP 300E spectrometer (Bruker) operating at X-band and equipped with a standard TE102 rectangular cavity. Computer simulations of the EPR spectra were performed with the help of *Simfonia* (Bruker) and *Winsim* (NIEH Public Software) software. Radical anions were generated by chemical oxidation with $AgSbF_6$ as the distilled solvent under an argon atmosphere or by electrolysis in a microcell set up in a 5-mm-inner-diameter quartz tube. Electrolyses were performed at controlled potential with a three-electrode configuration under an atmosphere of argon using a platinum wire as the working electrode, a platinum wire as the auxiliary electrode, and a silver wire as the pseudoreference electrode. A dilute solution (ca. 10^{-3} M) of the precursor neutral complex was prepared with $^{n}Bu_4NPF_6$ (10^{-1} M) as the supporting electrolyte.

■ ASSOCIATED CONTENT

Ⓢ Supporting Information

X-ray crystallographic data in CIF format, NMR spectra, HRMS spectra, X-ray structure crystal data, cyclic voltamogramms, and UV−visible and luminescence spectra. This material is available free of charge via the Internet at http://pubs.acs.org.

■ AUTHOR INFORMATION

Corresponding Authors

*E-mail: bellemin@unistra.fr.
*E-mail: dagorne@unistra.fr.

Notes

The authors declare no competing financial interest.

■ ACKNOWLEDGMENTS

We thank the CNRS and University of Strasbourg for financial support. C.R. acknowledges the MESR (French Ministry of

Research) for a Ph.D. fellowship. Prof. C. Lodeiro, Dr. E. Oliveira, and Dr. C. Nùñez (University of Nova, Lisbon, Portugal) are gratefully acknowledged for preliminary luminescence measurements.

REFERENCES

(1) Pugh, D.; Danopoulos, A. A. *Coord. Chem. Rev.* **2007**, *251*, 610.
(2) Hahn, F. E.; Jahnke, M. C. *Angew. Chem., Int. Ed.* **2008**, *47*, 3122.
(3) Herrmann, W. A. *Angew. Chem., Int. Ed.* **2002**, *41*, 1290.
(4) Bourissou, D.; Guerret, O.; Gabbaï, F. P.; Bertrand, G. *Chem. Rev.* **1999**, *100*, 39.
(5) César, V.; Bellemin-Laponnaz, S.; Gade, L. H. *Chem. Soc. Rev.* **2004**, *33*, 619.
(6) Crudden, C. M.; Allen, D. P. *Coord. Chem. Rev.* **2004**, *248*, 2247.
(7) de Frémont, P.; Marion, N.; Nolan, S. P. *Coord. Chem. Rev.* **2009**, *253*, 862.
(8) Kuppuswamy, S.; Ghiviriga, I.; Abboud, K. A.; Veige, A. S. *Organometallics* **2010**, *29*, 6711.
(9) Benhamou, L.; Chardon, E.; Lavigne, G.; Bellemin-Laponnaz, S.; César, V. *Chem. Rev.* **2011**, *111*, 2705.
(10) Mercs, L.; Albrecht, M. *Chem. Soc. Rev.* **2010**, *39*, 1903.
(11) Visbal, R.; Gimeno, M. C. *Chem. Soc. Rev.* **2014**.
(12) Liddle, S. T.; Edworthy, I. S.; Arnold, P. L. *Chem. Soc. Rev.* **2007**, *36*, 1732.
(13) Kühl, O. *Chem. Soc. Rev.* **2007**, *36*, 592.
(14) Bellemin-Laponnaz, S.; Welter, R.; Brelot, L.; Dagorne, S. *J. Organomet. Chem.* **2009**, *694*, 604.
(15) Dagorne, S.; Bellemin-Laponnaz, S.; Romain, C. *Organometallics* **2013**, *32*, 2736.
(16) Romain, C.; Brelot, L.; Bellemin-Laponnaz, S.; Dagorne, S. *Organometallics* **2010**, *29*, 1191.
(17) Romain, C.; Heinrich, B.; Bellemin-Laponnaz, S.; Dagorne, S. *Chem. Commun.* **2012**, *48*, 2213.
(18) Luca, O. R.; Crabtree, R. H. *Chem. Soc. Rev.* **2013**, *42*, 1440.
(19) Lyaskovskyy, V.; de Bruin, B. *ACS Catal.* **2012**, *2*, 270.
(20) Praneeth, V. K. K.; Ringenberg, M. R.; Ward, T. R. *Angew. Chem., Int. Ed.* **2012**, *51*, 10228.
(21) Chaudhuri, P.; Wieghardt, K. *Progress in Inorganic Chemistry*; John Wiley & Sons, Inc.: New York, 2002; p 151.
(22) Pierpont, C. G.; Lange, C. W. *Progress in Inorganic Chemistry*; John Wiley & Sons, Inc.: New York, 2007; p 331.
(23) Adam, B.; Bill, E.; Bothe, E.; Goerdt, B.; Haselhorst, G.; Hildenbrand, K.; Sokolowski, A.; Steenken, S.; Weyhermüller, T.; Wieghardt, K. *Chem.—Eur. J.* **1997**, *3*, 308.
(24) Lionetti, D.; Medvecz, A. J.; Ugrinova, V.; Quiroz-Guzman, M.; Noll, B. C.; Brown, S. N. *Inorg. Chem.* **2010**, *49*, 4687.
(25) Quiroz-Guzman, M.; Oliver, A. G.; Loza, A. J.; Brown, S. N. *Dalton Trans.* **2011**, *40*, 11458.
(26) Szigethy, G.; Heyduk, A. F. *Dalton Trans.* **2012**, *41*, 8144.
(27) Blackmore, K. J.; Ziller, J. W.; Heyduk, A. F. *Inorg. Chem.* **2005**, *44*, 5559.
(28) Blackmore, K. J.; Lal, N.; Ziller, J. W.; Heyduk, A. F. *Eur. J. Inorg. Chem.* **2009**, *2009*, 735.
(29) Munha, R. F.; Zarkesh, R. A.; Heyduk, A. F. *Dalton Trans.* **2013**, *42*, 3751.
(30) Pfennig, B. W.; Thompson, M. E.; Bocarsly, A. B. *J. Am. Chem. Soc.* **1989**, *111*, 8947.
(31) Pfennig, B. W.; Thompson, M. E.; Bocarsly, A. B. *Organometallics* **1993**, *12*, 649.
(32) Paulson, S.; Sullivan, B. P.; Caspar, J. V. *J. Am. Chem. Soc.* **1992**, *114*, 6905.
(33) Heinselman, K. S.; Hopkins, M. D. *J. Am. Chem. Soc.* **1995**, *117*, 12340.
(34) Kenney, J. W.; Boone, D. R.; Striplin, D. R.; Chen, Y. H.; Hamar, K. B. *Organometallics* **1993**, *12*, 3671.
(35) Wing-Wah Yam, V.; Qi, G.-Z.; Cheung, K.-K. *J. Chem. Soc., Dalton Trans.* **1998**, 1819.
(36) Yam, V. W.-W.; Qi, G.-Z.; Cheung, K.-K. *Organometallics* **1998**, *17*, 5448.
(37) Loukova, G. V.; Smirnov, V. A. *Chem. Phys. Lett.* **2000**, *329*, 437.
(38) Loukova, G. V.; Starodubova, S. E.; Smirnov, V. A. *J. Phys. Chem. A* **2007**, *111*, 10928.
(39) Pritchard, V. E.; Thorp-Greenwood, F. L.; Balasingham, R. G.; Williams, C. F.; Kariuki, B. M.; Platts, J. A.; Hallett, A. J.; Coogan, M. P. *Organometallics* **2013**, *32*, 3566.
(40) Koller, J.; Sarkar, S.; Abboud, K. A.; Veige, A. S. *Organometallics* **2007**, *26*, 5438.
(41) Golisz, S. R.; Labinger, J. A.; Bercaw, J. E. *Organometallics* **2010**, *29*, 5026.
(42) Agapie, T.; Henling, L. M.; DiPasquale, A. G.; Rheingold, A. L.; Bercaw, J. E. *Organometallics* **2008**, *27*, 6245.
(43) Tapu, D.; Dixon, D. A.; Roe, C. *Chem. Rev.* **2009**, *109*, 3385.
(44) Williams, D. S.; Korolev, A. V. *Inorg. Chem.* **1998**, *37*, 3809.
(45) Loukova, G. V.; Strelets, V. V. *J. Organomet. Chem.* **2000**, *606*, 203.
(46) Polo, E.; Barbieri, A.; Traverso, O. *New J. Chem.* **2004**, *28*, 652.